Fluidization of Mixtures of Two Solids Differing in Density or Size

B. Formisani, R. Girimonte, and V. Vivacqua
Dipartimento di Ingegneria Chimica e dei Materiali, Universita della Calabria, Arcavacata di Rende, Cosenza I 87030, Italy

DOI 10.1002/aic.12450
Published online November 29, 2010 in Wiley Online Library (wileyonlinelibrary.com).

The complex mechanism by which homogeneous mixtures of two solids achieve fluidization is subjected to theoretical analysis, to elaborate relationships capable to provide their "initial" and "final fluidization velocity" u_{if} *and* u_{ff}*, i.e., the limits that encompass the suspension process. The article shows how the equation that describes the force equilibrium of fluidization can be rewritten in forms that account for the distribution of the components of density- or size segregating mixtures during the transition to the fluidized state. This approach leads to the theoretical expression of* u_{if} *and* u_{ff} *of either type of system, whose differences of behavior are correctly reproduced by accounting for the voidage reduction typical of beds of particles of different size. The comparison with experimental results at varying mixture composition demonstrates that the equations give a coherent interpretation of the dependence of the fluidization velocity interval of two-solid mixtures on the principal variables of interest.* © 2010 American Institute of Chemical Engineers *AIChE J,* 57: 2325–2333, 2011
Keywords: fluidization, solids processing, mixing, mathematical modeling

Introduction

Although widely investigated in the last three decades, the fluidization properties of two-solid mixtures, the simplest type of multicomponent particle beds, constitute an area of fluidization research where theoretical achievements are still noticeably scarce.

The distinctive feature of binary fluidization is that particle suspension occurs simultaneously with the modification of the axial distribution of bed components, so that both phenomena are regulated by a complex mechanism whose variants are related to the properties of the solids that form the mixture. Even if these characteristics seem sufficient to explain the difficulty of modeling the process, this is likely to be also a consequence of the nature of the approach to the problem followed in most literature studies. Indeed, the prevailing attitude has been so far that of trying to extend to binary beds some fundamental concepts of the fluidization theory of monosolid systems. To this regard, many authors have tried to give a proper definition of the minimum fluidization velocity of a two-solid bed and various equations have been proposed to calculate u_{mf}.[1–7] Unfortunately, as these relationships are mostly empirical, their validity is usually limited to specific categories of mixtures.

As comprehensively discussed in a recent work,[8] however, any criterion aiming to establish an equivalence between a two-component bed and a monosolid system with the same u_{mf} gives place to a misleading approach, fated to overlook important aspects of the binary fluidization phenomenology. The most important of them is the gradual nature of the process, which results from the interaction between the progress of particle suspension and that of the segregation-remixing phenomena to which the two solids are subjected. Accordingly, a different method of analysis, hitherto followed by few other research groups,[8–12] has been proposed. On the ground of it, there is the idea that no incipient fluidization velocity can be defined with reference to a two-component bed, since its fluidization takes place along an extended

Correspondence concerning this article should be addressed to B. Formisani at bruno.formisani@unical.it.

Table 1. Independent Variables of Binary Fluidization

Solid properties	
Solid densities	ρ_f, ρ_j
Particle diameters	d_f, d_j
Particle shape factors	ϕ_f, ϕ_j
Mixture properties	
Composition	x_f
Bed voidage	ε
Fluidization velocity	U
Packed bed distribution	mixed, segregated (f/j or j/f), other

velocity interval whose boundaries are defined as the "initial" and the "final fluidization velocity" of the mixture, u_{if} and u_{ff}, respectively. A valuable characteristic of this approach is that it facilitates the identification of the variables that determine the fluidization pattern of the two-solid bed, as their variations are clearly reflected by a change of either u_{if} or u_{ff}. The number of these parameters, here listed in Table 1 after the aforementioned study, is rather large; that constitutes a serious complication for the development of a model of binary fluidization endowed with general validity.

On this way, an important intermediate objective is that of elaborating a theory capable to predict the initial and final fluidization velocities of a two-solid bed right from the knowledge of the constitutive properties of its components. It must be born in mind, to this regard, that the fluidization velocity interval of a mixture is also that in which its components display their tendency to segregate or, alternatively, to mix up, a behavior dictated also by their initial arrangement in the fixed bed. The value of u_{if} can thus be calculated in function of the axial distribution of the two solids in the packed state,[8] whereas the prediction of u_{ff} results much more complicated in that the final fluidization velocity results from the cross-action of fluidization and segregation phenomena. Even when the field of investigation is restricted to the behavior of homogeneous mixtures, as done in this study, the large number of variables to deal with sets a strong limit to the usefulness of empirical methods. As this article tries to demonstrate, a sounder choice is therefore that of addressing the problem of segregating fluidization in fundamental terms, so as to develop the potentialities of the approach followed in recent research.

Binary Fluidization Phenomenology

The mechanism by which a homogeneous mixture of two solids achieves fluidization is more complex than that of a monosolid system in that it develops along an extended velocity interval and is accompanied by segregation and remixing of system components.

As far as the behavior of free-flowing particles (belonging to Geldart Group B) is concerned, by progressively increasing the velocity of the gas flowing across the fixed bed a point is reached at which the flotsam particles located in the upper region of the bed are first fluidized and gather up in a thin bubbling layer while the jetsam ones, previously mixed with them, form a static layer underneath (Figure 1a). While it fixes the value of u_{if}, this event coincides with the appearance of a fluidization front which gradually shifts downwards in response to any further increase of the gas flow rate; at the same time, the total pressure drop starts to deviate from the curve typical of the fixed state. Subsequently, as much as u exceeds u_{if} a larger part of the system is involved in the suspension process and the two layers grow in thickness (Figure 1b) while, under them, the height of the region not yet reached by the fluidization front, i.e., the residual portion of the original mixture, decreases. Along with the increase of the gas velocity over u_{if}, the intensity of the bubbly flow through the flotsam layer grows and, consequently, the interface between the two layers becomes less and less distinct. Eventually, the whole mixture is suspended into the upflowing gas at u_{ff}, where the final pressure drop level is first attained; varying with the specific nature of the mixture as well as with its composition, the state of complete fluidization corresponds to a higher degree of component mixing (Figure 1c) even if a top layer of practically pure flotsam is always observed.

Notwithstanding some clear differences of behavior between density- and size-segregating mixtures, mainly relevant to the extent at which component segregation occurs during the suspension process, the essential features of the mechanism of fluidization of both types of beds are the same

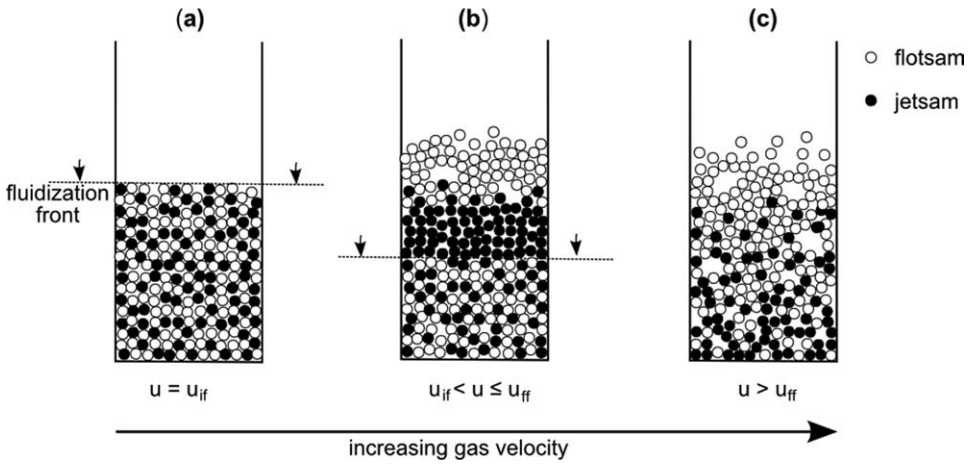

Figure 1. Fluidization mechanism of a homogeneous bed of two solids.

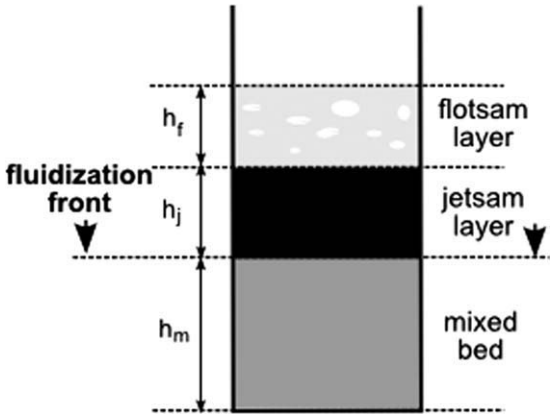

Figure 2. Idealized component distribution during the fluidization process.

in that two characteristic velocities, u_{if} and u_{ff}, are required to describe the transition of the system from the fixed to the fluidized state. That constitutes a major difference with the case of monosolid beds, for which the same event is associated to the definition of just one parameter, namely their minimum fluidization velocity u_{mf}.

For any representation of segregating fluidization, it is then indispensable setting up relationships for calculating the two boundaries of the fluidization velocity interval and validating them over a wide range of experimental conditions.

Theory

Theoretical equations for calculating the initial fluidization velocity of homogeneous mixtures of spheres of different density or diameter have already been proposed in previous papers.[8,13] To set up these relationships, a fundamental equation of fluidization like Carman-Kozeny's (or Ergun's, when mixture components are such that their u_{mf} falls out of the viscous regime) has been rewritten in forms suitable to account for the binary nature of the bed. Their predictive capacity has then been verified on a wide variety of data relevant to experiments carried out on mixtures of either type.

As regards two-density systems, u_{if} turns up to be the weighed average of the minimum fluidization velocities of the two components:

$$u_{if} = x_f u_{mf,f} + (1 - x_f) u_{mf,j} \tag{1}$$

to be calculated as

$$\frac{180\mu_g u_{if}}{d^2}\frac{(1-\varepsilon_{mf})^2}{\varepsilon_{mf}^3} = \left[(\rho_f-\rho_g)x_f + (\rho_j-\rho_g)(1-x_f)\right](1-\varepsilon_{mf})g \tag{2}$$

whereas for two-size systems it is calculated from the equation

$$\frac{180\mu_g u_{if}}{d_{av}^2}\frac{\left(1-\varepsilon_{mf,m}\right)^2}{\varepsilon_{mf,m}^3} = \left(\rho-\rho_g\right)\left(1-\varepsilon_{mf,m}\right)g \tag{3}$$

with the surface/volume average particle diameter given by the relationship

$$\frac{1}{d_{av}} = \frac{x_f}{d_f} + \frac{1-x_f}{d_j} \tag{4}$$

and the value of bed voidage $\varepsilon_{mf,m}$ drawn from the experimental curve of $\varepsilon_{mf,m}$ vs. x_f.

On the other hand, the final fluidization velocity of a two-solid mixture has been defined as the velocity at which the pressure drop across the bed attains its ultimate value,[8–10] a condition achieved when the weight of whole bed is sustained by the gas-solid drag.

To analyze the dependence of u_{ff} on composition and on the constitutive properties of the two solids, a force balance can be written. At any operating velocity intermediate to u_{if} and u_{ff}, the axial distribution of mixture components is approximately that sketched in Figure 2, an idealized version of Figure 1b with sharp interfaces between the three layers, whose heights are indicated as h_f, h_j, and h_m, respectively. Once the bed is reduced to this simplified structure, its fluidization dynamics can be analyzed by a force balance altogether similar to that typical of simple systems but written in a form capable to account for the interaction among the various parts of the system. By this method, the fluidization properties of both density-segregating and size-segregating mixtures can be addressed. However, a peculiar feature of the latter type of systems is that bed voidage depends on component diameter ratio and local composition.[14] For this reason, to understand and describe some essential differences of behavior between the two types of mixtures, a separate analysis is required, whose essential features are summarized, for the sake of clarity, in Table 2.

Density-segregating mixtures

The voidage of mixtures of spherical particles having the same average diameter but different densities does not significantly change with composition or axial component distribution.[8,13] Under this assumption (and neglecting the little error on h_f due to the presence of bubbles in the flotsam layer), when particle segregation is driven only by the difference in solid density, the total drag force on the three sections of the bed can be expressed as

$$F_d = \frac{180\mu_g u}{d^2}\frac{(1-\varepsilon_{mf})^2}{\varepsilon_{mf}^3}A\left(h_f + h_j + h_m\right) \tag{5}$$

and has to balance, at u_{ff}, the buoyant weight

$$W = (1-\varepsilon_{mf})gA\left\{\left(\rho_f-\rho_g\right)h_f + \left(\rho_j-\rho_g\right)h_j + \left[\left(\rho_f-\rho_g\right)x_f + \left(\rho_j-\rho_g\right)(1-x_f)\right]h_m\right\} \tag{6}$$

Table 2. Model Assumptions

- The segregation pattern of a well-mixed binary bed gives place to three distinct layers (pure flotsam, pure jetsam, residual mixture) of varying height;
- Bed voidage is:
  a) practically independent of composition for density-segregating mixtures;
  b) a function of d_f/d_j and x_f for size-segregating mixtures;
- The hold-up of bubbles in the flotsam layer does not significantly change its height;
- The fluidization process of pure mixture components is described by Carman-Kozeny (or Ergun) equation.

Given that since its formation at u_{if} the top layer of flotsam particles finds itself over its incipient fluidization point, at any velocity higher than u_{if} but lower than u_{ff} the condition

$$\frac{180\mu_g u}{d^2}\frac{(1-\varepsilon_{mf})^2}{\varepsilon_{mf}^3}Ah_f = (1-\varepsilon_{mf})gA(\rho_f-\rho_g)h_f \quad (7)$$

holds, so that equating Eqs. 5 and 6 provides the expression of u_{ff}:

$$u_{ff} = \frac{\{(\rho_j-\rho_g)h_j + [(\rho_f-\rho_g)x_f + (\rho_j-\rho_g)(1-x_f)]h_m\}g\varepsilon_{mf}^3 d^2}{180\mu_g(1-\varepsilon_{mf})(h_m+h_j)} \quad (8)$$

As far as ε_{mf} does not vary with layer composition, a mass balance on the jetsam shows that its segregated amount is related to the decrease of the height of the homogeneous portion of the binary bed occurred past u_{if}:

$$h_j = (h_0 - h_m)(1-x_f) \quad (9)$$

At the same time, the minimum fluidization velocity of either solids are calculated as

$$u_{mf,f_j} = \frac{(\rho_{f,j}-\rho_g)d^2\varepsilon_{mf}^3 g}{180\mu_g(1-\varepsilon_{mf})} \quad (10)$$

so that substitution of Eqs. 9 and 10 into 8 yields

$$u_{ff} = \frac{u_{mf,f}h_m x_f + u_{mf,j}h_0(1-x_f)}{h_m x_f + h_0(1-x_f)} \quad (11)$$

that expresses u_{ff} in function of the minimum fluidization velocity of either solid.

Equation 11 relates the upper boundary of the fluidization velocity interval of a mixture of known average composition to the quantitative effect of segregation up to the moment the gas drag force begins to support the whole bed mass. For a bed of initial height h_0, this effect is measured by h_m, the residual height of the original mixture left at the bottom of the bed.

Size-segregating mixtures

Unlike what is a distinctive feature of beds of particles of different density, namely the fact that system voidage is practically unaffected by any other variable, with two-size mixtures any change of composition or of the state of mixing of their components is followed by a variation of voidage. As a consequence of that, the progress of segregation phenomena induced by fluidization causes these beds to continuously change their axial profile of local voidage.

On rewriting Eq. 5 for this category of systems, it has therefore to be considered that the void fractions of the segregated layers of flotsam and jetsam of Figure 2 are higher than that of the binary assembly of composition x_f underneath, so that now

$$F_d = \frac{180\mu_g u}{d_f^2}\frac{(1-\varepsilon_{mf,f})^2}{\varepsilon_{mf,f}^3}Ah_f + \frac{180\mu_g u}{d_j^2}\frac{(1-\varepsilon_{mf,j})^2}{\varepsilon_{mf,j}^3}Ah_j + \frac{180\mu_g u}{d_{av}^2}\frac{(1-\varepsilon_{mf,m})^2}{\varepsilon_{mf,m}^3}Ah_m \quad (12)$$

As the two solids have the same density, the buoyant weight of the bed is

$$W = (\rho-\rho_g)gA[(1-\varepsilon_{mf,f})h_f + (1-\varepsilon_{mf,j})h_j + (1-\varepsilon_{mf,m})h_m] \quad (13)$$

and equating the two relationships after eliminating the terms relevant to the flotsam layer as done in Eq. 7 gives

$$u_{ff} = \frac{(\rho-\rho_g)g[(1-\varepsilon_{mf,j})h_j + (1-\varepsilon_{mf,m})h_m]}{180\,\mu_g\left[\frac{(1-\varepsilon_{mf,j})^2}{(\varepsilon_{mf,j}^3 d_j^2)}h_j + \frac{(1-\varepsilon_{mf,m})^2}{(\varepsilon_{mf,m}^3 d_{av}^2)}h_m\right]} \quad (14)$$

Given that the voidage of the segregated jetsam layer is different from that of the residual binary bed under it, the mass balance on this component is now

$$h_j = (h_0 - h_m)(1-x_f)\frac{(1-\varepsilon_{mf,m})}{(1-\varepsilon_{mf,j})} \quad (15)$$

Thus, substitution of Eq. 15 together with the expressions (10) of $u_{mf,f}$ and $u_{mf,j}$ into (14) yields

$$u_{ff} = \frac{u_{mf,f}\frac{(1-\varepsilon_{mf,f})}{(\varepsilon_{mf,f}^3 d_f^2)}h_m x_f + u_{mf,j}\frac{(1-\varepsilon_{mf,j})}{(\varepsilon_{mf,j}^3 d_j^2)}h_0(1-x_f)}{\frac{(1-\varepsilon_{mf,m})}{(\varepsilon_{mf,m}^3 d_{av}^2)}h_m + \frac{(1-\varepsilon_{mf,j})}{(\varepsilon_{mf,j}^3 d_j^2)}(h_0-h_m)(1-x_f)} \quad (16)$$

that relates the final fluidization velocity of the mixture to the properties of its components.

Parametric correlation for the ratio h_m/h_0

As it is not easy, for the time being, to establish a reliable relationship between the progress of binary fluidization from u_{if} to u_{ff} and the variation of the height h_m of the residual homogeneous mixture, a correlation has been devised to interpretate data relevant to both density- and size-segregating beds:

$$\frac{h_m}{h_0} = k\frac{(1-\varepsilon_{mf,m})}{(1-\varepsilon_{mf,j})}\frac{\varepsilon_{mf,j}^3}{\varepsilon_{mf,m}^3}\sqrt{x_f(1-x_f)} \quad (17)$$

In it, h_m is the residual height of the homogeneous mixture at its final fluidization velocity and k is a fitting parameter typical of each mixture but independent of its composition, to be determined from the comparison of the predictions of the theoretical Equation (11) or (16) with the experimental curves of u_{ff} vs. x_f.

The height ratio h_m/h_0 in Eq. 17 is a measure of the tendency of the mixture to remain, at u_{ff}, in the homogeneous

Table 3. Properties of the Experimental Solids and Mixtures

Solid	Density (g/cm^3)	Sieve size (μm)	Sauter mean diameter (μm)	Minimum fluidization velocity (cm/s)
Molecular sieves (MS)	1.46	600–710	624	20.8
Glass ballotini (GB)	2.48	600–710	631	32.5
		500–710	593	30.8
		350–600	499	20.2
		400–500	428	17.9
		250–300	271	5.7
		200–250	223	4.3
		150–180	172	2.8
		125–180	154	2.2
Ceramics (CE)	3.76	500–710	605	43.3
Steel shots (SS)	7.60	400–500	439	47.7
		200–250	243	17.3

Type	Mixture	ρ_j/ρ_f (–)	$\rho_j - \rho_f$ (g/cm^3)	d_j/d_f (–)	ε_{mf} (–)	k (–)
Density-segregating	CE605–GB593	1.52	1.28	1.02	0.405	0.39
	GB593-MS624	1.70	1.02	0.95	0.410	0.69
	SS439-GB428	3.06	5.12	1.03	0.426	0.21
	SS243-GB223	3.06	5.12	1.09	0.430	0.42
Size-segregating	GB631-GB154	1	–	4.10	see Figure 6	0.077
	GB499-GB172	1	–	2.90	see Figure 6	0.18
	GB499-GB271	1	–	1.84	see Figure 6	0.70

state; this seems related to the gain in drag force effectiveness provided by the void condition typical of the mixed state,[7] expressed by the ratio

$$\frac{\left(1-\varepsilon_{mf,m}\right)}{\left(1-\varepsilon_{mf,j}\right)}\frac{\varepsilon_{mf,j}^3}{\varepsilon_{mf,m}^3}$$

Equation 17 has therefore to be looked at as a relationship that links these variables to a function of mixture composition capable to give the best fit of data.

Values of voidage relevant to the pure jetsam component ($\varepsilon_{mf,j}$) and to the mixture ($\varepsilon_{mf,m}$) are taken from the experiments and substituted into Eq. 17. Depending on whether the components of the bed differ in density or size, $\varepsilon_{mf,m}$ results practically constant with x_f or varies with mixture composition. With the former type of beds, made of spheres of the same size, whatever the composition the difference between $\varepsilon_{mf,j}$ and $\varepsilon_{mf,m}$ is practically negligible so that the voidage function in the right hand side of Eq. 17 may always be assumed equal to 1.

Experimental

The results analyzed in this work come from series of experiments performed in a transparent column with an internal diameter of 10 cm. Compressed air, whose flow rate was measured by a bench of rotameters, was admitted to the facility through a plastic porous plate 4 mm thick, capable to ensure even distribution throughout the column section. A pressure tap located 1 mm above the distributor and connected to a U-tube water manometer was used to measure the total pressure drop across the bed, while three graduated scales spaced at 120° around the column wall allowed determining the average bed height at any velocity level. Such measurements were used to calculate the initial fixed-bed voidage from the relationship

$$\varepsilon_0 = 1 - \frac{m}{\rho A h_0} \tag{18}$$

so as to reconstruct its dependence on the volumetric fraction of the flotsam component.

All the experiments were performed on well-mixed binary mixtures. To ensure homogeneity of the fixed bed, each mixture was fractioned into various portions (6 to 8) each of which was mechanically premixed and then poured onto the column by means of a long-legged funnel. The effectiveness of this procedure, validated by previous work, was checked by occasionally determining the axial profile of bed composition according to a method described in detail in a previous work [8].

Given that the investigation is based on mixtures of solids included in Geldart's group B, the fixed bed voidage ε_0 calculated by Eq. 18 has always been assumed to be equal to the minimum fluidization voidage ε_{mf}, after verification that the error connected to this procedure was negligible.

Closely sieved cut of various spherical materials were used throughout the experimental campaign; their granulometric characterization was performed by a Malvern Mastersizer 2000 laser diffractometer, while a Quantachrome helium pycnometer was employed for density measurements. Table 3 reports both the properties of the various solids and those of the two-component systems used in the experiments. With all mixtures the aspect ratio h_0/D of the fixed bed was set equal to 1.7, so that their composition was varied by adjusting the mass of their components under this constraint.

Validation of the Model

The ability of the theory proposed in this article to interpretate the fluidization behavior of binary mixtures affected by either of the two driving forces of segregation (the density or size difference between components) can be evaluated by comparing the values of u_{if} and u_{ff} drawn from experiments at varying x_f with those calculated by the model

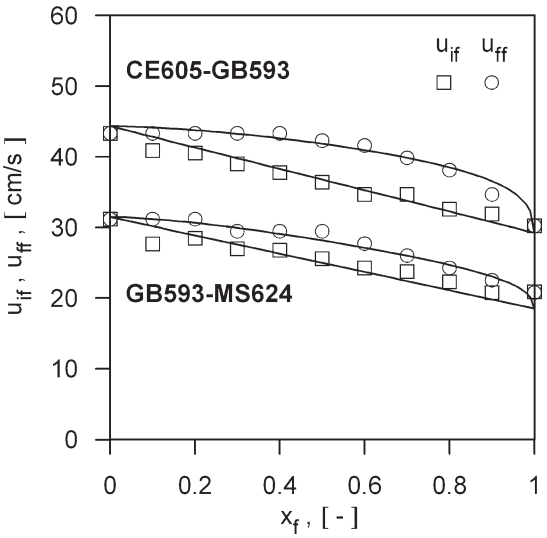

Figure 3. Fluidization velocity diagram of the density-segregating mixtures CE605-GB593 and GB593-MS624.

equations. Over the whole range of composition, the two series of values provide the general fluidization diagram of each system, either in the experimental or in the calculated version. On it, at any concentration, the vertical distance between the curve of u_{ff} and that of u_{if} represents the width of the velocity interval along which the binary bed is entirely brought into the fluidized state. During this process, its internal component distribution goes through a succession of equilibrium states, each of which is typical of the specific value of u.

Unlike the model curves of u_{if}, obtained from the theoretical equations (2) and (3), those of u_{ff} are derived from relationships, namely the equations (11) and (16) that cannot be looked at as fully predictive. In either of them the presence of h_m (the height of the homogeneous portion of the bed at the final fluidization condition) requires the association of Eq. 17, in which the value of k is that capable to provide the best fit of the experimental data over the whole field of x_f.

Density-segregating mixtures

In Figures 3 and 4, the initial and the final fluidization velocity of four density-segregating binary beds are plotted vs. the volumetric fraction of their flotsam component. The density ratio of their solids ranges from 1.52 to 3.06 covering nearly all the situations encountered in the applications of two-component fluidization. The properties of these systems, as well as those of the size-segregating mixtures referred to later on in this section, are reported in Table 3.

As already observed in previous investigations,[8,13] in the experimental fluidization diagram of two-density mixtures u_{if} is given by the straight line joining component u_{mf}'s and modeled by Eq. 1 or 2, whereas the locus of u_{ff} is a curve whose slope progressively increases with x_f.

From the experimental viewpoint, the fluidization diagrams of the two-density systems considered demonstrate that the dependence on x_f of both characteristic velocities is not a function of the solid density ratio ρ_j/ρ_f but is dictated by the difference $u_{mf,j} - u_{mf,f}$. This difference is related, in turn, to the difference $\rho_j d_j^2 - \rho_f d_f^2$, as stated by Eq. 10. Thus, the amplitude of the fluidization velocity intervals of mixtures CE605-GB593 and SS243-GB223, which have a component density ratios of 1.52 and 3.06 but u_{mf} differences of 12.5 and 13.0, respectively, results practically identical at all compositions (Figures 3 and 4). At the same time, the fluidization diagrams of SS243-GB223 and SS439-GB428 reported in Figure 4 exhibit a substantial difference of amplitude, that corresponds to a difference in component u_{mf} equal to 13.0 and 29.8, respectively. That occurs notwithstanding that the ratio ρ_j/ρ_f is equal to 3.06 for both systems. As for the mixture GB593-MS624, its fluidization diagram appears to be the narrowest of all without its density ratio, equal to 1.70, being the smallest.

The fitting procedure of the experimental curves of u_{ff} with the Eqs. 11 and 17 provides the values of the parameter k, also reported in Table 3, to be used in the latter relationship at all compositions. In it, as well as in Eq. 2, $\varepsilon_{mf,m}$ can be assumed practically constant with x_f, with a negligible error. Average values of $\varepsilon_{mf,m}$, drawn from the measurements performed on each binary assembly, are reported in Table 3 as well. The role played by the difference $u_{mf,j} - u_{mf,f}$ in the binary fluidization process is successfully reflected by the model parameter k, whose values result very close for mixtures CE605-GB593 and SS243-GB223 (0.39 and 0.42, respectively) whereas they are noticeably different for SS243-GB223 and SS439-GB428 (0.42 and 0.21, respectively), where a smaller difference in component u_{mf} corresponds to a higher value of k.

The ability of the theory proposed in Sec. 3 to interpret the binary fluidization pattern is illustrated by the comparison between experimental and calculated values of u_{ff}: as observable in Figure 5, the error of prediction always falls within the limit of 10%.

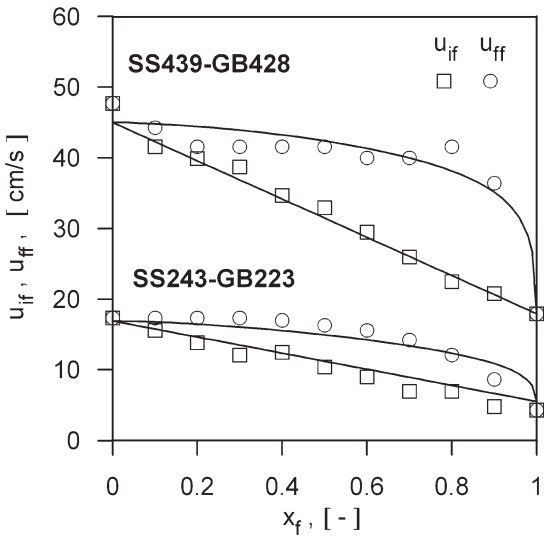

Figure 4. Fluidization velocity diagram of the density-segregating mixtures SS439-GB428 and SS243-GB223.

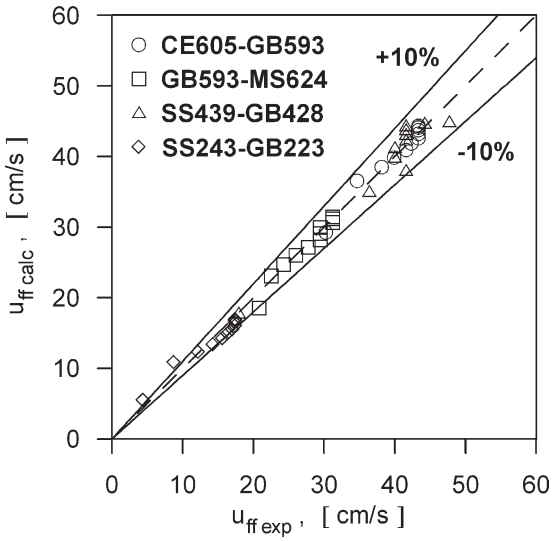

Figure 5. Comparison between experimental and calculated values of the final fluidization velocity. Density-segregating mixtures.

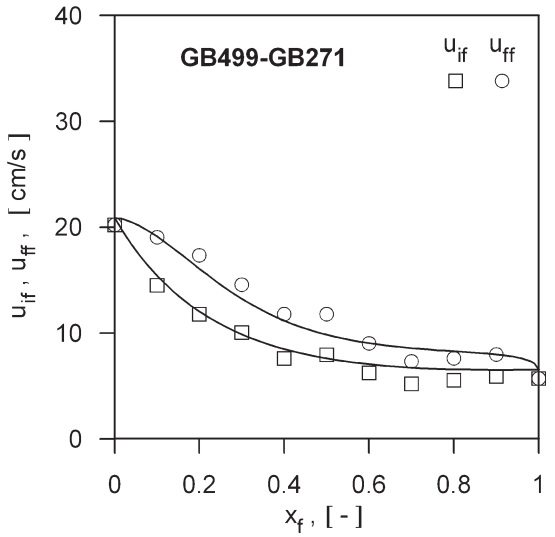

Figure 7. Fluidization velocity diagram of the size-segregating mixture GB499-GB271.

Size-segregating mixtures

As a major difference with the case of two-density mixtures, the voidage of binary beds whose segregation tendency is due to the difference of component diameters varies with their composition.[8,12,14] As for the systems investigated in this article (GB499-GB271, GB499-GB172, and GB631-GB154), the experimental dependence of $\varepsilon_{mf,m}$ on x_f is plotted in Figure 6. Values of $\varepsilon_{mf,m}$ drawn from these curves have been used when applying Eq. 3 to predict the initial fluidization velocity u_{if} of these mixtures (a point already treated in a recent paper[8]), and Eqs. 16 and 17 to fit the experimental data of their u_{ff}.

The fluidization velocity diagrams of these systems are plotted in Figures 7–9, together with the relevant model curves. Both the initial and the final fluidization velocity exhibit curvilinear trends at varying x_f, determined by both the difference $u_{mf,j} - u_{mf,f}$ and the peculiar shape of the $\varepsilon_{mf,m}$ vs. x_f curve, in turn determined by the particle size ratio d_j/d_f.[8,14]

Notwithstanding that the complication associated to the voidage change introduces a new variable into the problem of segregating fluidization, the ability of the model equations to represent the dependence of u_{ff} on x_f once that the value of k has been defined, is remarkable. For the three mixtures under scrutiny k results equal to 0.70, 0.18, and 0.077, respectively, so that it diminishes when the component size ratio of the mixture d_j/d_f grows (see Table 3). Similar to what observed with density-segregating systems, a general comparison between experimental and calculated values of u_{ff}, carried out in Figure 10, confirms that the error is generally lower than 10%.

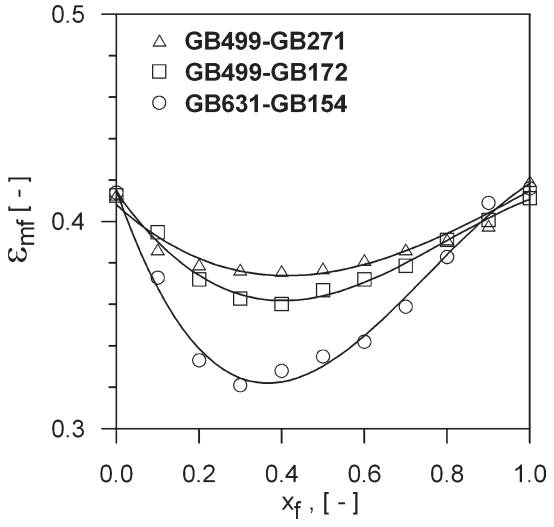

Figure 6. Voidage of homogeneous size-segregating mixtures at varying composition.

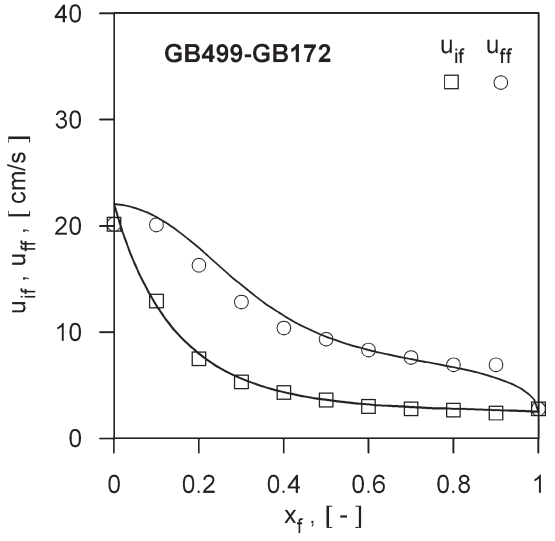

Figure 8. Fluidization velocity diagram of the size-segregating mixture GB499-GB172.

Discussion

On setting up a theory for calculating the two boundaries of the fluidization velocity interval of a two-solid mixture, a result of previous investigations has been retrieved, i.e., that at all compositions Eqs. 2 and 3–4 allow predicting u_{if} from the knowledge of the constitutive properties of mixture components and of bed voidage, namely the same amount of information required for predicting u_{mf} of a monosolid bed. As regards instead u_{ff}, the necessity of drawing from the experiments the value of the parameter k to be used in Eq. 17 still prevents a model like that proposed in this article from being equally predictive.

In front of this apparent limitation, to be overcome by a deeper insight into the mechanisms of particle segregation, stands out the overall ability of the model to interpretate the dependence of the amplitude of the fluidization velocity field of a binary mixture, namely the difference $u_{ff} - u_{if}$, on the variables it is function of (component density and diameter, composition, voidage, etc.). For the case of density-segregating beds, subtracting Eq. 1 from 11 yields, after rearrangement:

$$(u_{ff} - u_{if}) = \frac{(h_0 - h_m)(1 - x_f)x_f}{h_m + (h_0 - h_m)(1 - x_f)}\left(u_{mf,j} - u_{mf,f}\right) \quad (19)$$

By applying the same procedure to size-segregating mixtures, i.e., by working out the result obtained by subtracting Eq. 3 from 16, a corresponding relationship can be written,

$$(u_{ff} - u_{if}) = \frac{\frac{\varepsilon_{mf,m}^3}{\varepsilon_{mf,j}^3}\frac{\left(1-\varepsilon_{mf,j}\right)}{\left(1-\varepsilon_{mf,m}\right)}\frac{d_{av}^2}{d_j^2}(h_0 - h_m)(1 - x_f)}{h_m + \frac{\varepsilon_{mf,m}^3}{\varepsilon_{mf,j}^3}\frac{\left(1-\varepsilon_{mf,j}\right)}{\left(1-\varepsilon_{mf,m}\right)}\frac{d_{av}^2}{d_j^2}(h_0 - h_m)(1 - x_f)} \times \left(u_{mf,j} - \frac{\varepsilon_{mf,m}^3}{\varepsilon_{mf,f}^3}\frac{\left(1-\varepsilon_{mf,f}\right)}{\left(1-\varepsilon_{mf,m}\right)}\frac{d_{av}^2}{d_f^2}u_{mf,f}\right), \quad (20)$$

whose apparent complexity is entirely due to the terms that account for the dependence of voidage on system composition.

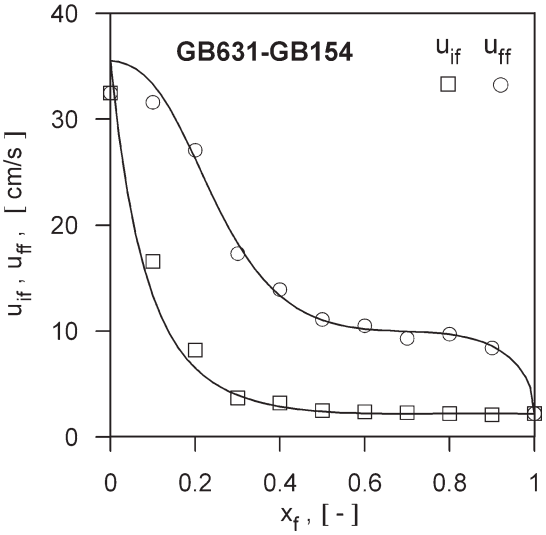

Figure 9. Fluidization velocity diagram of the size-segregating mixture GB631-GB154.

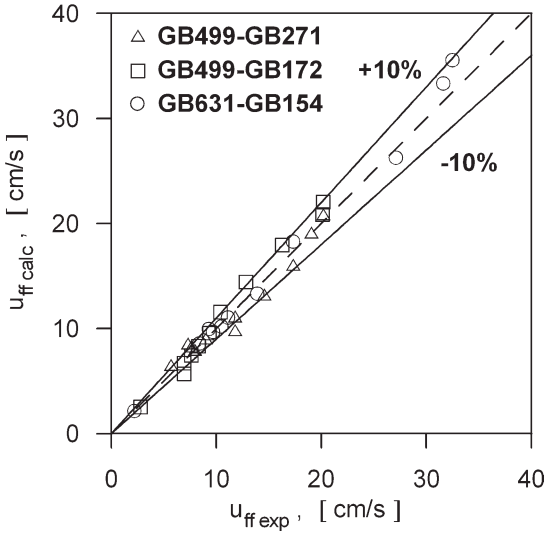

Figure 10. Comparison between experimental and calculated values of the final fluidization velocity. Size-segregating mixtures.

Thus, through the analysis of the behavior of homogeneous systems, this study confirms the possibility of addressing the problem of segregating fluidization in fundamental terms.

As a fruit of this approach, Eqs. 11 and 16 not only give evidence that the final fluidization velocity of all mixtures is always lower than u_{mf} of their jetsam component but also successfully interpretate the variation of u_{ff} with composition. A crucial point, to this regard, seems that of applying the force balance to a realistic structure: in spite of some evident simplifications, like that of considering the equilibrium state of the two-solid bed to give rise to three distinct layers of definite composition and height, the scheme of Figure 2 proves capable to represent the essential aspects of the suspension mechanism. It is worth noticing, for instance, that the condition at which the weight of the mixture is balanced by the total pressure drop, first achieved at u_{ff}, occurs before the fluidization front has crossed the whole height of the bed, a circumstance confirmed by visual observation of the experiments.

The most valuable achievement of the present investigation is probably that implicit in the fact that Eq. 17 can be used with both types of mixtures without any difference in the error level of Figures 5 and 10. That demonstrates that application of the fundamental theory makes possible a unique description of segregating fluidization, regardless of the driving force of segregation being the inequality of particle density or size. Out of some other minor effects, a clear evidence has been given that the main difference of behavior between two-density and two-size mixtures arises from the voidage variation experienced by the latter in response to any change in local composition, an added complication in that it introduces a new variable into the phenomenology. Once that this aspect of the problem is properly accounted for, the need for a separated analysis of the behavior of density- and size-segregating mixtures is therefore eliminated. This has to be looked at as a novel result in the field, likely to be extensible to mixtures of dissimilar materials and such

to encourage new efforts toward a fully theoretical model of segregating fluidization.

Conclusions

Modeling the fluidization pattern of homogeneous beds of two solids subjected to either density or size segregation can successfully be undertaken in fundamental terms if the actual phenomenology of the process is correctly accounted for.

The transition to the fluidized condition has place gradually, along a velocity interval bounded by the initial and final fluidization velocity of the mixture. The succession of equilibrium states crossed by the binary bed in the passage from u_{if} to u_{ff} is associated to a peculiar distribution of its components, subjected to continuous evolution and close to a three-layer structure. Fundamental analysis of the forces acting on these particle layers provides the theoretical expressions of u_{ff} (11) and (16), valid for density- and size-segregating mixtures, respectively. Coupled with the equations for calculating u_{if} set up in previous studies, these relationships give a correct interpretation of the dependence of the width of the fluidization velocity interval on variables such as solid density and size, mixture composition, average system voidage and bed height. However, calculation of u_{ff} requires the knowledge of the height of the residual portion of homogeneous bed at the endpoint of the fluidization process, a variable related to the strength of the segregation tendency in the binary bed. In the absence of a fully predictive theory of segregation, this can be estimated by a simple one-parameter equation, valid for both types of segregating mixtures.

Notation

A = column cross section (cm^2)
D = bed diameter (cm)
d = particle diameter (μm)
d_{av} = Sauter mean diameter (Eq. 4) (μm)
F_d = drag force (g cm/s^2)
g = gravity acceleration (cm/s^2)
h = height of the particle layer (cm)
h_0 = height of the fixed bed (cm)
k = best-fit parameter (Eq. 17)
m = bed mass (g)
u_{if}, u_{ff} = initial, final fluidization velocity (cm/s)
u_{mf} = minimum fluidization velocity (cm/s)
x = volume fraction
W = buoyant weight of the bed (g cm/s^2)
ε_0 = fixed bed voidage (–)
ε_{mf} = minimum fluidization voidage (–)
μ_g = gas viscosity (g/cm s)
ϕ = particle sphericity (–)
ρ = solid density (g/cm^3)
ρ_g = gas density (g/cm^3)

Subscripts

$_{f,j}$ = of the flotsam, jetsam component (or layer)
$_m$ = of the homogeneous mixture

Literature Cited

1. Otero AR, Corella J. Fluidizacion de mezclas de solidos de distintas caracteristicas. *An R Soc Esp Fis y Quim*. 1971;67:1207–1219.
2. Goossens WRA, Dumont GL, Spaepen GL. Fluidization of binary mixtures in the laminar flow region. *AIChE Symp Ser*. 1971;67:38–45.
3. Cheung L, Nienow AW, Rowe PN. Minimum fluidisation velocity of a binary mixture of different sized particles. *Chem Eng Sci*. 1974;29:1301–1303.
4. Chiba S, Chiba T, Nienow AW, Kobayashi H. The minimum fluidisation velocity, bed expansion and pressure-drop profile of binary particle mixtures. *Powder Technol*. 1979;22:255–269.
5. Thonglimp V, Hiquily N, Laguerie C. Vitesse minimale de fluidisation et expansion des couches de mélanges de particules solides fluidisées par un gaz. *Powder Technol*. 1984;39:223–239.
6. Noda K, Uchida S, Makino T. Kamo H. Minimum fluidization velocity of binary mixtures of particles with large size ratio. *Powder Technol*. 1986;46:149–154.
7. Formisani B. Packing and fluidization properties of binary mixtures of spherical particles. *Powder Technol*. 1991;66:259–264.
8. Formisani B, Girimonte R, Longo, T. The fluidization process of binary mixtures of solids: development of the approach based on the fluidization velocity interval. *Powder Technol*. 2008;185:97–108.
9. Chen JL-P, Keairns DL. Particle segregation in a fluidized bed. *Can J Chem Eng*. 1975;53:395–402.
10. Vaid RP, Sen Gupta P. Minimum fluidization velocities in beds of mixed solids. *Can J Chem Eng*. 1978;56:292–296.
11. Carski M, Pata J, Vesely V, Hartman M. Binary system fluidized bed equilibrium, *Powder Technol*. 1987;51:237–242.
12. Olivieri G, Marzocchella A, Salatino P. Segregation of fluidized binary mixture of granular solids. *AIChE J*. 2004;50:3095–3106.
13. Formisani B, Girimonte R, Longo, T. The fluidization pattern of density-segregating binary mixtures. *Chem Eng Res Des*. 2008;86:344–348.
14. Yu AB, Standish N. Porosity calculations of multi-component mixtures of spherical particles. *Powder Technol*. 1987;52:233–241.

Manuscript received Nov. 10, 2009, and revision received Sep. 7, 2010.